

Journal of Materials Chemistry B

Accepted Manuscript



This is an *Accepted Manuscript*, which has been through the Royal Society of Chemistry peer review process and has been accepted for publication.

Accepted Manuscripts are published online shortly after acceptance, before technical editing, formatting and proof reading. Using this free service, authors can make their results available to the community, in citable form, before we publish the edited article. We will replace this *Accepted Manuscript* with the edited and formatted *Advance Article* as soon as it is available.

You can find more information about *Accepted Manuscripts* in the [Information for Authors](#).

Please note that technical editing may introduce minor changes to the text and/or graphics, which may alter content. The journal's standard [Terms & Conditions](#) and the [Ethical guidelines](#) still apply. In no event shall the Royal Society of Chemistry be held responsible for any errors or omissions in this *Accepted Manuscript* or any consequences arising from the use of any information it contains.

Cite this: DOI: 10.1039/c0xx00000x

www.rsc.org/xxxxxx

ARTICLE

A colorimetric and ratiometric fluorescent probe for ClO⁻ targeting on mitochondria and the application in *in vivo*

Hongde Xiao^a, Jianhui Li^a, Jin Zhao^b, Gui Yin^{a,c*}, Yiwu Quan^a, Jie Wang^a and Ruiyong Wang^{b*}

Received (in XXX, XXX) Xth XXXXXXXXX 20XX, Accepted Xth XXXXXXXXX 20XX

DOI: 10.1039/b000000x

A colorimetric and ratiometric fluorescent probe PMN-TPP for imaging mitochondrial ClO⁻ was prepared. The selectivity of PMN-TPP was excellent, and the detection would not be influenced by other ROS. The limit of detection (LOD=3σ/Slope) towards ClO⁻ was evaluated to be 0.43 μM, suggesting the probe's high sensitivity to ClO⁻. For the biological applicants, PMN-TPP performed well in detecting endogenous HClO in the living RAW264.7 macrophage cells. Co-localization study employing Mito Tracker green revealed that PMN-TPP was specifically located in the mitochondria of the living RAW264.7 macrophage cells. In the *in vivo* experiment, nude mouse with acute inflammation stimulated by lipopolysaccharide (LPS) was employed. After injection of PMN-TPP, the fluorescent signal changed gradually in 30 min and then remained changeless in the injection region, demonstrating PMN-TPP could detect the endogenous HClO in living animals.

Introduction

Reactive oxygen species (ROS) have emerged as prevalent and important components of both physiological and pathological processes.¹ As a type of ROS, hypochlorous acid (HClO) and its conjugate base hypochlorite (ClO⁻) are widely employed as strong oxidizing agents in our daily life. In living organisms, the hypochlorite is produced mainly from hydrogen peroxide and chloride ions in a heme enzyme myeloperoxidase (MPO)-catalyzed reaction.² This is associated with innate host defence and is very important for killing a wide range of pathogens.³ As the major consumers of cellular oxygen, mitochondria play a central role in ROS biology. The foremost function of mitochondria is to produce ATP, the major energy currency molecule of the cell. The process of producing ATP involves a series of electron-transport systems in the oxidation phosphorylation pathway, which is ascribed to be associated with the generation of reactive oxygen species (ROS).⁴ Thus, maintenance of appropriate level of HClO in mitochondria is fairly crucial for numerous cellular functions. However, abnormal overproduction of HClO is considered to be associated with some diseases, such as rheumatoid arthritis and even cancers.⁵

^aState Key Laboratory of Analytical Chemistry for Life Science, School of Chemistry and Chemical Engineering, Nanjing University, Nanjing 210093, People's Republic of China, E-mail: yingui@nju.edu.cn

^bSchool of Life Science, Nanjing University, Nanjing, 210093, China
Email: wangry@nju.edu.cn

^cJiangsu Key Laboratory of Advanced Catalytic Materials and Technology, Changzhou University, 213164, China

Therefore, detecting mitochondrial HClO attracted extensive interests, especially taking advantages of fluorescent imaging techniques due to their high sensitivity, selectivity, rapid response rate and easiness of manipulating.⁶

However, even though a number of fluorescent probes detecting HClO have been developed,⁷ and applied to the *in vitro* and *in vivo* imaging of HClO,⁸ only a very limited amount of mitochondria-targeted fluorescent probes have been reported.⁹ And most of those fluorescent probes merely added a triphenylphosphonium (TPP) moiety or quaternized pyridine moiety, which have been utilized as mitochondria-targeted functional groups,¹⁰ to the formerly reported probes.¹¹ Moreover, as far as biological applications were concerned, those mitochondria-targeted probes merely detected exogenous HClO, hence the mitochondrial target did not make any sense in this condition. Furthermore, as far as we know, the reported mitochondria-targeted fluorescent probes are all of the "turn-on" type which only responds to HClO only in the fluorescence signal intensity. Unfortunately, in most practical applications, changes measured in the fluorescence intensity can also be affected by other variables such as the concentration of the probe molecule, the micro-environmental conditions or differences in optical components between instruments. Therefore, ratiometric fluorescent probes that can overcome the limitations of intensity-based probes and provide quantitative measurements via self-calibration of two emission bands are highly desirable.¹² Therefore, it is highly desirable to develop the water-soluble mitochondria-targeted ratiometric fluorescent probes for endogenous HClO; especially none of such kind of probe has been reported. In this study, we synthesized a highly water-soluble colorimetric and ratiometric fluorescent probe PMN-TPP to detect endogenous HClO in mitochondria of living RAW264.7 macrophage cells and the living nude mouse. The probe was prepared via a simple process and characterized using ¹H,

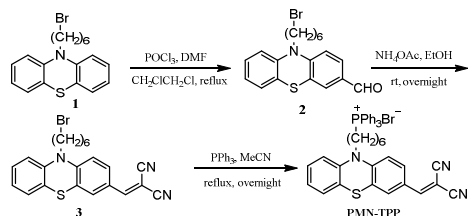
¹³CNMR and HR–MS.

Experiment

Equipments

¹H NMR and ¹³C NMR spectra were recorded on Bruker Ultrashield 300 MHz NMR spectrometer. Chemical shifts were expressed in ppm (in DMSO-d₆; TMS as internal standard) and coupling constants (*J*) in Hz. Mass spectroscopy was obtained from SHIMADZU LCMS-2020 and Agilent Technologies 6540 UHD Accurate-Mass Q-TOF LC/MS. Fluorescence spectra were measured using Hitachi Fluorescence spectrophotometer-F-4600. Absorption spectra were measured on a Perkin Elmer Lambda 35 UV/VIS spectrophotometer. Fluorescent images were captured by Olympus FV-1000 laser scanning confocal fluorescence microscope. Imaging of living mouse was conducted employing Perkin Elmer IVIS Lumina Spectrum Imaging System.

Synthesis



Scheme 1 synthesis of the probe PMN–TPP

Synthesis of the compound 2

To a 250-mL three-necked round-bottom flask containing N-methylformamide (1.62 g, 12 mmol) was added phosphorus oxychloride (2.30 g, 15 mmol) by dropwise. The mixture was stirred at room temperature under N₂ for 30 min. Then the mixture was added to a solution of 1 (3.62 g, 10 mmol) in 20 mL 1,2-dichloroethane by dropwise, and the reaction mixture was stirred at 85 °C under N₂ atmosphere for 6 h. After cooling to the room temperature, the mixture was poured in to ice water slowly, and then neutralized with 0.1 M NaOH. Afterwards, the mixture was extracted with dichloromethane (3×50 mL). The extractions were combined, washed with distilled water, saturated brine, and then dried over anhydrous sodium sulfate. After evaporation of solvent, the crude compound was purified over silica gel column and desired compound was eluted by PE: EA (10:1 v/v) to obtain 2.93 g pure product as yellow solid. Yield: 75 %. ¹H NMR (300 MHz, DMSO-d₆) δ 9.77 (s, 1H), 7.76 – 7.65 (m, 1H), 7.58 (d, *J* = 1.4 Hz, 1H), 7.21 (t, *J* = 7.7 Hz, 1H), 7.14 (d, *J* = 7.0 Hz, 2H), 7.06 (d, *J* = 8.1 Hz, 1H), 6.98 (t, *J* = 7.4 Hz, 1H), 3.92 (t, *J* = 6.8 Hz, 2H), 3.51 (dt, *J* = 31.2, 6.6 Hz, 2H), 1.70 (dd, *J* = 23.8, 6.6 Hz, 4H), 1.38 (d, *J* = 3.1 Hz, 4H). ¹³C NMR (75 MHz, DMSO-d₆) δ 190.98, 150.49, 143.44, 131.31, 130.59, 128.40, 128.23,

127.98, 127.72, 124.06, 123.04, 116.99, 116.00, 47.33, 35.37, 32.58, 27.51, 26.36, 25.57.

50

Synthesis of the compound 3

Compound 2 (482 mg, 2 mmol), malononitrile (132 mg, 2 mmol) and a catalytic amount of NH₄OAc were mixed in the mixture of 5 mL THF with 15 mL ethanol. The mixture was stirred at room temperature overnight. After evaporation of solvent, the crude compound was purified over silica gel column and desired compound was eluted by PE: EA (5:1 v/v) to obtain 3 (779 mg, 1.77 mmol) as a dark red solid. Yield: 88 %. ¹H NMR (300 MHz, DMSO-d₆) δ 8.23 (s, 1H), 7.81 (dd, *J* = 8.8, 2.0 Hz, 1H), 7.66 (d, *J* = 2.0 Hz, 1H), 7.29 – 7.06 (m, 4H), 7.01 (t, *J* = 7.4 Hz, 1H), 3.93 (t, *J* = 6.9 Hz, 2H), 3.52 (dt, *J* = 30.9, 6.6 Hz, 2H), 1.92 – 1.56 (m, 4H), 1.39 (d, *J* = 3.3 Hz, 4H). ¹³C NMR (75 MHz, DMSO-d₆) δ 159.19, 150.39, 142.50, 132.29, 129.34, 128.58, 127.75, 125.85, 124.51, 123.47, 122.18, 117.11, 116.06, 115.42, 114.53, 76.42, 47.49, 35.38, 32.60, 27.51, 26.29, 25.52.

Synthesis of the probe PMN–TPP

Compound 3 (437 mg, 1 mmol) and triphenylphosphine (2.62 g, 0.01 mol) were mixed in 15 mL acetonitrile. The mixture was heated to reflux overnight and was then cooled to room temperature. After evaporation of solvent, the crude compound was purified over silica gel column and desired compound was eluted by EA:MeOH (10:1 v/v) to obtain PMN–TPP (328 mg, 0.53 mmol) as a dark red solid. Yield: 53 %. HR–MS: *m/z* 620.2289 [M–Br]⁺ (calcd. 620.2289). ¹H NMR (300 MHz, DMSO-d₆) δ 8.26 (s, 1H), 7.94 – 7.83 (m, 3H), 7.84 – 7.68 (m, 14H), 7.65 (d, *J* = 1.9 Hz, 1H), 7.17 – 6.99 (m, 4H), 3.90 (t, *J* = 6.2 Hz, 2H), 3.56 (s, 2H), 1.60 (s, 2H), 1.39 (d, *J* = 40.0 Hz, 6H). ¹³C NMR (75 MHz, DMSO-d₆) δ 159.25, 150.40, 142.51, 135.37, 134.11, 133.98, 132.31, 130.78, 130.61, 129.35, 128.63, 127.78, 125.88, 124.56, 123.46, 122.15, 119.55, 118.41, 117.21, 116.18, 115.41, 114.58, 76.46, 47.43, 29.78, 29.56, 26.05, 25.47, 22.01, 20.92, 20.25.

Cell culture

RAW264.7 macrophage cells were cultured in Dulbecco's modified Eagle's medium (DMEM) containing 10% fetal bovine serum and antibiotics (100 units/mL penicillin and 100 μg/mL streptomycin), maintaining at 37 °C in a humidified atmosphere of 95% air and 5% CO₂.

Cell imaging

Fresh stock of RAW264.7 macrophage cells was seeded into a glass bottom dish with a density of 1×10⁵ cells per dish, and incubated for 24 h. In the control group, the cells were exposed to 10 μM PMN–TPP solution for 10 min at room temperature. The solution was then removed, and the cells were washed with PBS (2 mL×3) to clear PMN–TPP molecules attached to the surface of cells. Meanwhile, in the experiment group, after the macrophage cells have been incubated with LPS (1 μg/mL) for 5 h, and then

further coincubated with PMA (1 $\mu\text{g}/\text{mL}$) and PMN-TPP (5 μM) for 10 min. The culture medium was removed, and the treated cells were washed three times with PBS (2 mL \times 3) before observation. Fluorescence imaging was performed with confocal laser scanning microscopy (Olympus, FV-1000; λ_{ex} =405 nm).

Fluorescence Imaging in Living Mouse

A nude mouse (20–25 g) was given a skin-pop injection of LPS (100 $\mu\text{L}\times$ 1 $\mu\text{g}/\text{mL}$). After 12 h, PMA was injected to the same region. 30 min later, the mouse was anesthetized by inhalation of isoflurane. Then a solution of the probe PMN-TPP (20 $\mu\text{M}\times$ 50 μL in saline, containing 1% DMSO) was injected to the same region. As a control, unstimulated mouse given a skin-pop injection only with the probe PMN-TPP (20 $\mu\text{M}\times$ 50 μL in saline, containing 1% DMSO) were also prepared. The pictures were taken after the mouse was incubated for 0, 5, 10, 15, 20, 30, 45 and 60 min, respectively. All experiments were performed in compliance with the Regulations for the Administration of Affairs Concerning Experimental Animals published by Bureau of Legislative Affairs of the State Council of the People's Republic of China and guidelines of State Key Laboratory of Pharmaceutical Biotechnology in Nanjing University, and in addition, the institutional committee(s) approved the experiments.

Results and discussion

Fluorescence response of the probe PMN-TPP to different ROS

First, we explored whether the probe PMN-TPP could selectively detect ClO^- among the ROS including H_2O_2 , OH^- , O^{2-} , $^t\text{BuOOH}$, NO , ONOO^- . To the solution of PMN-TPP (100 μM) in PBS buffer (pH 7.3, 10 mM, containing 1% DMSO), various species of ROS were added respectively. As shown in Fig.1.b, upon addition of ClO^- (10 equiv), colour of the solution changed from light brown to colorless (inert of Fig. 3), accompanying the absorption peak at 468 nm decreased. However, addition of other ROS (100 equiv) had little effect on the absorption spectra. On the other hand, as far as the fluorescent property was concerned, various species of ROS were added to the solution of PMN-TPP (5 μM) in PBS buffer (pH 7.3, 10 mM, containing 1% DMSO and 1mM Triton X-100) respectively. Triton X-100 was introduced to form micellar systems to restrict the influence of the water to the PMN-TPP molecules, preventing quench of the fluorescence¹³. As shown in Fig.1.a, the solution of 5 μM PMN-TPP in PBS buffer emitted strongly at 640 nm upon excitation at 410 nm and showed red fluorescence upon excitation at 365 nm employing a hand-hold UV lamp. Addition of 25 μM ClO^- induced a great blue shift of the fluorescent peak from 640 nm to 522 nm. And the fluorescence also changed to yellow upon excitation at 365 nm using a hand-hold UV lamp (inert of Fig. 2). However, other species of ROS (500 μM) caused negligible influence to the fluorescence of the probe. Therefore, PMN-TPP was qualified to selectively detect ClO^- among the various competitive ROS.

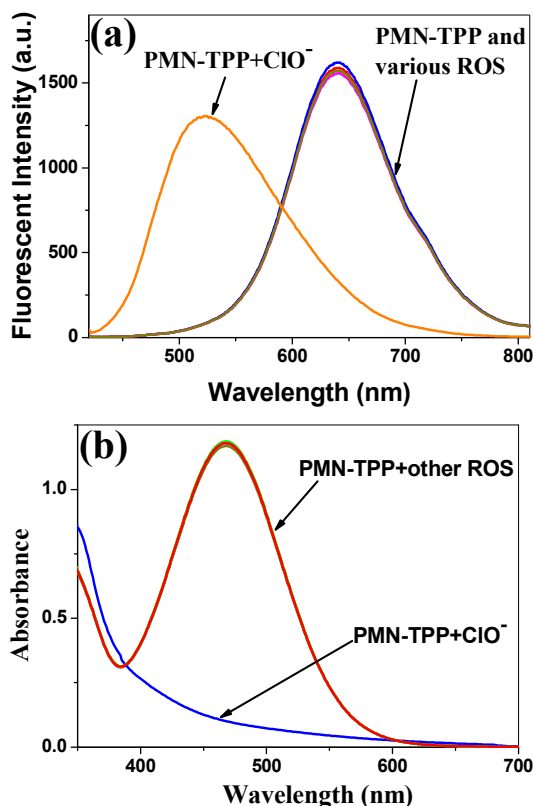


Fig. 1 (a) Fluorescence spectra of PMN-TPP (5 μM) at 562 nm before and after addition of various ROS in PBS (pH 7.3, 10 mM, containing 0.5 % DMSO and 1 mM Triton X-100). $[\text{ClO}^-] = 50 \mu\text{M}$, $[\text{OH}^-] = [\text{ONOO}^-] = [\text{O}^{2-}] = [^t\text{BuOOH}] = [\text{H}_2\text{O}_2] = [\text{NO}] = 500 \mu\text{M}$; (b) Absorption spectra of PMN-TPP (100 μM) at 562 nm before and after addition of various ROS in PBS (pH 7.3, 10 mM, containing 1% DMSO). $[\text{ClO}^-] = 1 \text{ mM}$, $[\text{OH}^-] = [\text{ONOO}^-] = [\text{O}^{2-}] = [^t\text{BuOOH}] = [\text{H}_2\text{O}_2] = [\text{NO}] = 10 \text{ mM}$.

Fluorescence titrations experiment

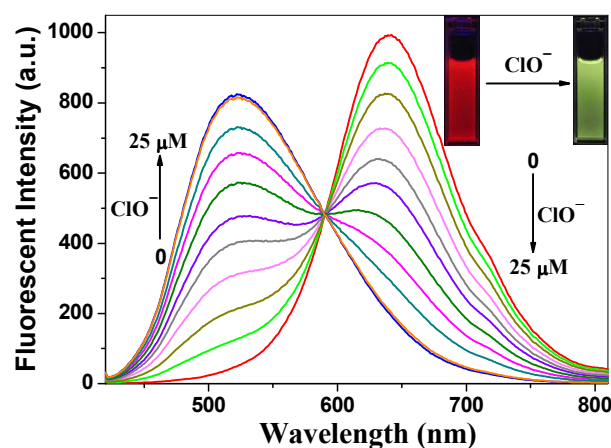


Fig.2 Fluorescence titration spectra of PMN-TPP (5 μM) upon addition of NaClO (0, 2.5, 5, 7.5, 10, 12.5, 15, 17.5, 20, 22.5, 25 μM) in PBS (pH 7.3, 10 mM, containing 0.5% DMSO and 1mM Triton X-100) upon excitation at 410 nm.

Then, the fluorescence titrations of the probe PMN-TPP (5 μM)

with ClO^- were conducted in PBS buffer (pH 7.3, 10 mM, containing 0.5% DMSO and 1 mM triton X-100). As shown in Fig. 2, the fluorescence intensity at 640 nm decreased gradually upon addition of ClO^- . Meanwhile, an emitting peak locating at 522 nm increased gradually. After 4.5 equiv. NaClO was added, the fluorescence remained changeless. The whole recognition process finished within just few seconds and remained nearly changeless over time. Such a short response time was due to the construction of micellar systems by Triton X-100 which offered a microenvironment to accelerate the observed rates of some chemical reactions.¹⁴ Thus, the real-time detection of ClO^- could be achieved employing PMN-TPP. To evaluate the limit of detection (LOD= $3\sigma/\text{Slope}$, σ is standard deviation) towards ClO^- , linear fitting of fluorescence intensity ratios at 522 and 640 nm ($I_{522\text{nm}}/I_{640\text{nm}}$) with the concentration of ClO^- was depicted in Fig. S1. The limit of detection was calculated to be 0.43 μM , demonstrating the high sensitivity of the probe towards ClO^- .

Absorption titration experiments

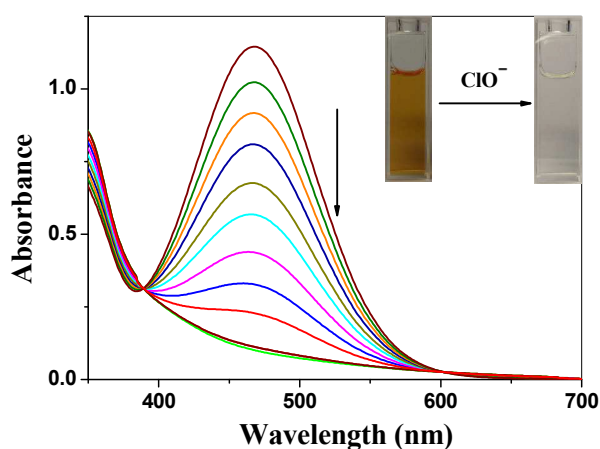
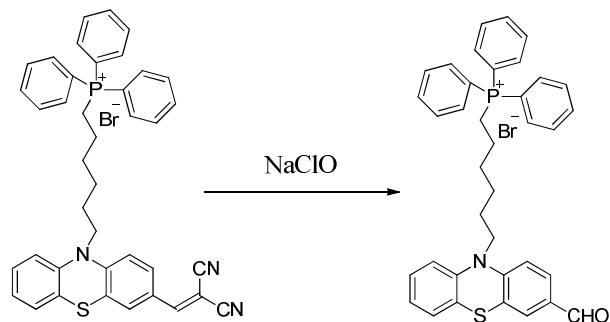


Fig. 3 Absorption spectra of the probe PMN-TPP (100 μM) upon additions of NaClO (0, 0.5, 1, 1.5, 2, 2.5, 3, 3.5, 4, 4.5, 5 equiv.) in PBS (pH 7.3, 10 mM, containing 1% DMSO).

Moreover, the changes of the UV-vis spectra of the probe in the absence and presence of ClO^- were then investigated. As shown in Fig. 3, the probe showed a main absorption band at 468 nm, which was due to the intramolecular charge transfer (ICT) transition in the molecule. Upon addition of ClO^- , the absorption peak of the probe at 468 nm decreased gradually, symbolizing the change of the conjugate structure. Fig. S2 showed a good linear fitting of the absorbance of the probe versus concentration of ClO^- (0–4.5 equiv). Moreover, the absorbance of the probe remained changeless after 4.5 equiv was added (Fig. S2), symbolizing the total consumption of the probe.

Investigation of the detecting mechanism



Scheme 2 The proposed reaction of PMN-TPP with ClO^- .

In organic reaction, the carbon-carbon double bond could be destroyed by oxidants. Thus, we suspected that the carbon-carbon double bond of the probe PMN-TPP might be cleaved upon the oxidation of ClO^- and the fluorescence changed as the decrease of the conjugate structure. To confirm our assumption, the reaction solution of PMN-TPP with ClO^- was analyzed by ESI-MS (Fig. S3). The prominent peak at m/z 572.10 corresponding to the aldehyde in Scheme 2 (calculated to be 572.22) was found in MS spectra, implying the production of the aldehyde.

The effect of pH

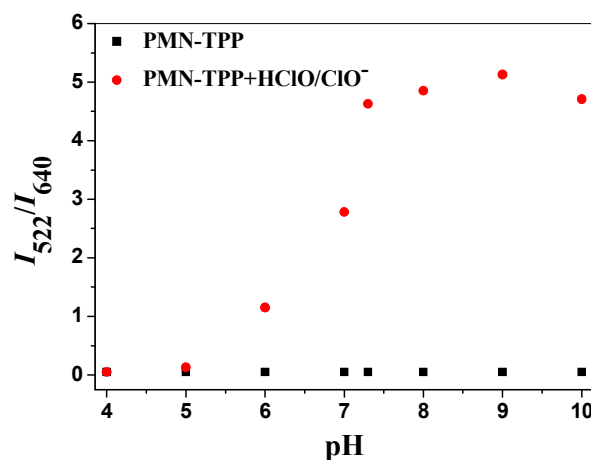


Fig. 4 The effect of pH values on the ratio of fluorescence intensity ratios at 522 and 640 nm of PMN-TPP (5 μM) in the absence or presence of ClO^- (25 μM). λ_{ex} = 400 nm; λ_{em} = 562 nm.

Furthermore, to test the application extent of the PMN-TPP as ClO^- probe, we next evaluated the fluorescent properties of the probe and its ability to react with HClO/ClO^- in a series of buffers with different pH values ranging from 4 to 10. As shown in Fig. 4, the probe detected ClO^- rather than HClO . Moreover, when the value of pH is 7.3, the probe performed well, indicating

PMN–TPP is compatible with most biological applications.

Investigation of the sub-cellular localization of PMN–TPP

To examine whether the probe PMN–TPP can target and specifically stain the mitochondria, Mito Tracker green, a widely used commercially available mitochondrial dye, was employed for a co-localization study (Fig. 5). As depicted in Fig. 5.e, the changes in the intensity profiles of linear regions of interest (ROIs) (the probe PMN–TPP and Mito Tracker Green co-staining) were synchronous, the fluorescent signals of the probe PMN–TPP overlaid well with the fluorescence of Mito Tracker Green. Moreover, co-localization was qualified using Pearson's sample correlation factors (Rr). The intensity of correlation plot (Fig. 5.f) revealed a high Pearson's coefficient (0.94), confirming that PMN–TPP was well cell-permeated and specifically located in the mitochondria of the living RAW264.7 macrophage cells.

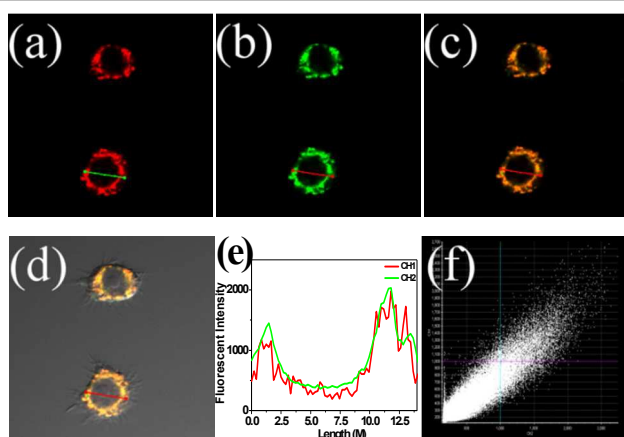


Fig. 5 (a–d) Confocal fluorescence images of RAW 264.7 cells. The cells were incubated with PMN–TPP (5 μM), and Mito Tracker Green (100 nM) for 20 min. (a) emission from the red channel, $\lambda_{\text{ex}}=405$ nm, λ_{em} : 531–590 nm; (b) emission from the green channel (mitochondrial staining, $\lambda_{\text{ex}}=488$ nm, λ_{em} : 500–530 nm); (c) merged image of a and b; (d) merged image of c and bright-field image. (e) Intensity profile of ROIs across RAW 264.7 cells. Red lines represent the intensity of the probe PMN–TPP and blue lines represent the intensity of Mito Tracker Green. (f) Correlation plot of Mito Tracker Green and PMN–TPP intensities.

Imaging of intracellular ClO^-

The desirable fluorescence properties of PMN–TPP for HClO prompted us to utilize it for the detection of intracellular endogenous HClO. When stimulated by lipopolysaccharide (LPS) and phorbol myristate acetate (PMA), macrophages may produce endogenous HClO¹⁵. MTT assay revealed that cell viability was rarely changed when 5 μM PMN–TPP was added for 24 h (Fig. S4). In the control group, the living RAW264.7 macrophage cells were incubated with PMN–TPP (5 μM) in culture medium for 10 min at 37 $^{\circ}\text{C}$, and exhibited strong red fluorescence. Whereas in the experiment group, after the macrophage cells have been incubated with LPS (0.5 $\mu\text{g}/\text{mL}$) for 5 h, and then further coincubated with PMA (0.5 $\mu\text{g}/\text{mL}$) and PMN–TPP (5 μM) for

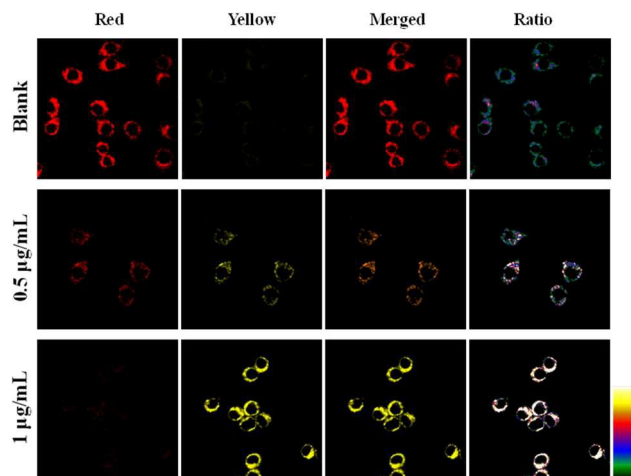


Fig. 6 Confocal fluorescence images of PMN–TPP–stained RAW 264.7 cells upon stimulation by LPS and PMA with varied concentration. Rows from top to bottom: blank, 0.5 $\mu\text{g}/\text{mL}$ LPS and 0.5 $\mu\text{g}/\text{mL}$ PMA, 1 $\mu\text{g}/\text{mL}$ LPS and 1 $\mu\text{g}/\text{mL}$ PMA. Columns from left to right: red channel, yellow channel, overlay of red and yellow channel, and ratio image, respectively. Images were acquired using 405 nm excitation and fluorescent emission filter: red: 630–650 nm, yellow: 510–530 nm.

10 min, the fluorescence of the red channel weakened and the fluorescence of the yellow channel turned on. On the other hand, for the macrophage cells which have been incubated with LPS (1 $\mu\text{g}/\text{mL}$) for 5 h, and then further coincubated with PMA (1 $\mu\text{g}/\text{mL}$) and PMN–TPP (5 μM) for 10 min, the fluorescence of the red channel nearly disappeared and the yellow fluorescence became very strong. The ratio picture also confirmed that the fluorescence intensity ratios of yellow channel and red channel increased. The aforementioned phenomena showed that PMN–TPP was capable of imaging endogenous HClO in the living RAW264.7 macrophage cells.

Imaging endogenous HClO *in vivo*

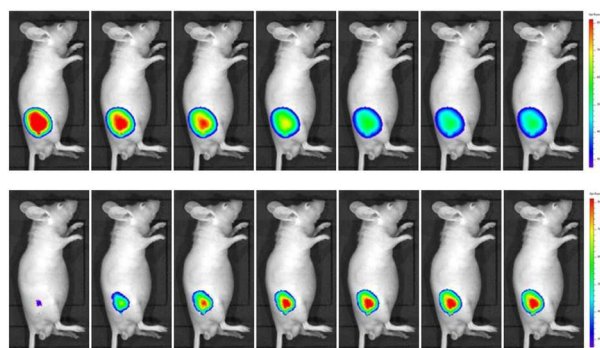


Fig. 7 Representative fluorescence images (pseudocolor) of a nude mouse. The mouse was given a skin-pup injection of LPS (100 $\mu\text{L}\times 1$ $\mu\text{g}/\text{mL}$) for 12 h, then an injection of PMA (50 $\mu\text{L}\times 1$ $\mu\text{g}/\text{mL}$) for 30 min, finally a skin-pup injection of PMN–TPP (50 $\mu\text{L}\times 20$ μM). Images were taken after incubation for 0, 5, 10, 15, 20, 30, 45 and 60 min, respectively. Images were taken using an excitation laser of 430 nm and an emission filter of DsRed channel.

We then evaluated the suitability of the probe for imaging endogenous HClO in living animals. The HClO produced *in vivo* was generated by activated macrophages and neutrophils in a lipopolysaccharide (LPS) model of acute inflammation¹⁶. In this case, nude mice were selected as our model. A solution of LPS (100 $\mu\text{L} \times 1 \mu\text{g}/\text{mL}$) was injected into the back of the mouse, and 12 hours later, PMA (50 $\mu\text{L} \times 1 \mu\text{g}/\text{mL}$) was then injected into the same region. After 30 min of the above disposal, the probe (50 $\mu\text{L} \times 20 \mu\text{M}$ in saline, containing 1% DMSO) was injected into the same region. The pictures were taken under the imaging system after the mouse was treated for 0, 5, 10, 15, 20, 30, 45 and 60 min, respectively. As shown in Fig. 7, the fluorescence signal obtained through the DsRed channel weakened gradually as the time went by. Whereas for the GFP channel, intensity of the fluorescence signal increased gradually, symbolizing that the probe reacted with the endogenous HClO in the nude mouse. The result established that PMN–TPP was a desired probe for imaging endogenous HClO *in vivo*.

Conclusions

In summary, a colorimetric and ratiometric fluorescent probe PMN–TPP for ClO^- was developed. The probe exhibited excellent selectivity towards ClO^- over other ROS with high sensitivity. Detections of intracellular ClO^- were conducted employing living RAW264.7 macrophage cells. The probe could target on mitochondria successfully taking advantage of the triphenylphosphonium (TPP) unit. Finally, the probe was applied in the *in vivo* detection of endogenous ClO^- using living nude mouse.

Acknowledgments

This work was supported by the National Natural Science Foundation of China (No. 21174061), National Basic Research Program of China (No. 2014CB846004), Jiangsu Key Laboratory of Advanced Catalytic Materials and Technology (No. BM2012110) and Jiangsu Province Science Technology Innovation and Achievements Transformation Special Fund (BY2012149).

Notes and references

- (a) J. R. Stone and S. Yang, *Antioxid Redox Sign*, 2006, **8**, 243; (b) B. DAutrEaux and M. B. Toledano, *Nat. Rev. Mol. Cell Biol.*, 2007, **8**, 813; (c) C. C. Winterbourn, *Nat. Chem. Biol.*, 2008, **4**, 278.
- (a) J. E. Harrison and J. Schultz, *J. Biol. Chem.*, 1976, **251**, 1371; (b) Y. W. Yap, M. Whiteman and N. S. Cheung, *Cell. Signalling*, 2007, **19**, 219.
- Z. M. Prokopowicz, F. Arce, R. Biedron, C. L. L. Chiang, M. Ciszek, D. R. Katz, M. Nowakowska, S. Zapotoczny, J. Marcinkiewicz and B. M. Chain, *J. Immunol.*, 2010, **184**, 824.
- (a) A. T. Hoye, J. E. Davoren, P. Wipf, M. P. Fink, V. E. Kagan, *Acc. Chem. Res.*, 2008, **41**, 87; (b) C. W. T. Leung, Y. N. Hong, S. J.

- Chen, E. G. Zhao, J. W. Y. Lam and B. Z. Tang, *J. Am. Chem. Soc.*, 2013, **135**, 62.
- (a) A. Daugherty, J. L. Dunn, D. L. Rateri and J. W. Heinecke, *J. Clin. Invest.*, 1994, **94**, 437; (b) S. M. Wu and S. V. Pizzo, *Arch. Biochem. Biophys.*, 2001, **391**, 119; (c) S. Weitzman and L. Gordon, *Blood*, 1990, **76**, 655.
- (a) H. D. Xiao, K. Chen, N. N. Jiang, D. D. Cui, G. Yin, J. Wang, R. Y. Wang, *Analyst*, 2014, **139**, 1980; (b) G. K. Vegesna, J. Janjanam, J. H. Bi, F. T. Luo, J. T. Zhang, *J. Mater. Chem. B*, 2014, **2**, 4500; (c) S. L. Zhu, J. T. Zhang, J. Janjanam, G. Vegesna, F. T. Luo, A. Tiwari and H. Y. Liu, *J. Mater. Chem. B*, 2013, **1**, 1722.
- (a) S. Kenmoku, Y. Urano, H. Kojima and T. Nagano, *J. Am. Chem. Soc.*, 2007, **129**, 7313; (b) X. Chen, X. Wang, S. Wang, W. Shi, K. Wang and H. Ma, *Chem.–Eur. J.*, 2008, **14**, 4719; (c) Y. K. Yang, H. J. Cho, J. Lee, I. Shin and J. Tae, *Org. Lett.*, 2009, **11**, 859; (d) G. Chen, F. Song, J. Wang, Z. Yang, S. Sun, J. Fan, X. Qiang, X. Wang, B. Dou and X. J. Peng, *Chem. Commun.*, 2012, **48**, 2949.
- (a) B. Wang, P. Li, F. Yu, P. Song, X. Sun, S. Yang, Z. Lou and K. L. Han, *Chem. Commun.*, 2013, **49**, 1014; (b) Z. Lou, P. Li, Q. Pan and K. L. Han, *Chem. Commun.*, 2013, **49**, 2445; (c) Z. R. Lou, P. Li, P. Song and K. L. Han, *Analyst*, 2013, **138**, 6291.
- (a) G. H. Cheng, J. L. Fan, W. Sun, K. Sui, X. Jin, J. Y. Wang and X. J. Peng, *Analyst*, 2013, **138**, 6091; (b) J. T. Hou, M. Y. Wu, K. Li, J. Yang, K. K. Yu, Y. M. Xie and Xi. Q. Yu, *Chem. Commun.*, 2014, **50**, 8640; (c) H. D. Xiao, K. Xin, H. Dou, G. Yin, Q. Yiwu and R. Y. Wang, *Chem. Commun.*, 2015, **51**, 1442.
- (a) A. T. Hoye, J. E. Davoren and P. Wipf, *Acc. Chem. Res.*, 2008, **41**, 87; (b) E. M. Nolan, J. W. Ryu, J. Jaworski, R. P. Feazell, M. Sheng and S. J. Lippard, *J. Am. Chem. Soc.*, 2006, **128**, 15517.
- (a) M. Emrullahoglu, M. Uçuncu and E. Karakus, *Chem. Commun.*, 2013, **49**, 7836; (b) X. Q. Chen, X. C. Wang, S. J. Wang, W. Shi, K. Wang and H. M. Ma, *Chem. – Eur. J.*, 2008, **14**, 4719.
- C. M. Yu, Y. L. Wu, F. Zeng and S. Z. Wu, *J. Mater. Chem. B*, 2013, **1**, 4152.
- G. P. Li, D. J. Zhu, Q. Liu, L. Xue and H. Jiang, *Org. Lett.*, 2013, **15**, 924.
- (a) R. Zana, *Adv. Colloid Interface Sci.*, 2002, **97**, 205; (b) D. Torsten, E. Paetzold, G. Oehme, *Angew. Chem., Int. Ed.*, 2005, **44**, 7174.
- X. Q. Chen, X. Z. Tian, I. Shin and J. Yoon, *Chem. Soc. Rev.*, 2011, **40**, 4783.
- K. Kundu, F. Knight, N. Willett, S. Lee, W. R. Taylor, N. Murthy, *Angew. Chem. Int. Ed.*, 2009, **48**, 299.

A colorimetric and ratiometric fluorescent probe PMN-TPP for imaging mitochondrial ClO^- was prepared. The probe performed well in detecting ClO^- in mitochondria of the living RAW264.7 macrophage cells and nude mouse.

